



AFRL-RY-WP-TR-2017-0164

INTEGRATED MAGNETO-OPTICAL DEVICES FOR ON-CHIP PHOTONIC SYSTEMS

Caroline Ross and Juejun Hu

Massachusetts Institute of Technology

**SEPTEMBER 2017
Final Report**

Approved for public release; distribution is unlimited.

See additional restrictions described on inside pages

STINFO COPY

**AIR FORCE RESEARCH LABORATORY
SENSORS DIRECTORATE
WRIGHT-PATTERSON AIR FORCE BASE, OH 45433-7320
AIR FORCE MATERIEL COMMAND
UNITED STATES AIR FORCE**

NOTICE AND SIGNATURE PAGE

Using Government drawings, specifications, or other data included in this document for any purpose other than Government procurement does not in any way obligate the U.S. Government. The fact that the Government formulated or supplied the drawings, specifications, or other data does not license the holder or any other person or corporation; or convey any rights or permission to manufacture, use, or sell any patented invention that may relate to them.

This report is the result of contracted fundamental research deemed exempt from public affairs security and policy review in accordance with SAF/AQR memorandum dated 10 Dec 08 and AFRL/CA policy clarification memorandum dated 16 Jan 09. This report is available to the general public, including foreign nationals.

Copies may be obtained from the Defense Technical Information Center (DTIC) (<http://www.dtic.mil>).

AFRL-RY-WP-TR-2017-0164 HAS BEEN REVIEWED AND IS APPROVED FOR PUBLICATION IN ACCORDANCE WITH ASSIGNED DISTRIBUTION STATEMENT.

// Signature//

DALE M. STEVENS
Program Manager
RF/EO Subsystems Branch
Aerospace Components & Subsystems Division

// Signature//

TIMOTHY R. JOHNSON, Chief
RF/EO Subsystems Branch
Aerospace Components & Subsystems Division

// Signature//

TODD W. BEARD, Lt Col, USAF
Deputy
Aerospace Components & Subsystems Division
Sensors Directorate

This report is published in the interest of scientific and technical information exchange, and its publication does not constitute the Government's approval or disapproval of its ideas or findings.

*Disseminated copies will show “//Signature//” stamped or typed above the signature blocks.

REPORT DOCUMENTATION PAGE

*Form Approved
OMB No. 0704-0188*

The public reporting burden for this collection of information is estimated to average 1 hour per response, including the time for reviewing instructions, searching existing data sources, gathering and maintaining the data needed, and completing and reviewing the collection of information. Send comments regarding this burden estimate or any other aspect of this collection of information, including suggestions for reducing this burden, to Department of Defense, Washington Headquarters Services, Directorate for Information Operations and Reports (0704-0188), 1215 Jefferson Davis Highway, Suite 1204, Arlington, VA 22202-4302. Respondents should be aware that notwithstanding any other provision of law, no person shall be subject to any penalty for failing to comply with a collection of information if it does not display a currently valid OMB control number. **PLEASE DO NOT RETURN YOUR FORM TO THE ABOVE ADDRESS.**

1. REPORT DATE (DD-MM-YY) September 2017			2. REPORT TYPE Final		3. DATES COVERED (From - To) 3 May 2016 – 3 May 2017	
4. TITLE AND SUBTITLE INTEGRATED MAGNETO-OPTICAL DEVICES FOR ON-CHIP PHOTONIC SYSTEMS			5a. CONTRACT NUMBER FA8650-16-1-7641			
			5b. GRANT NUMBER			
			5c. PROGRAM ELEMENT NUMBER 62716E			
6. AUTHOR(S) Caroline Ross and Juejun Hu			5d. PROJECT NUMBER N/A			
			5e. TASK NUMBER N/A			
			5f. WORK UNIT NUMBER Y1G1			
7. PERFORMING ORGANIZATION NAME(S) AND ADDRESS(ES) Massachusetts Institute of Technology 77 Massachusetts Avenue Cambridge, MA 02139-4301			8. PERFORMING ORGANIZATION REPORT NUMBER			
9. SPONSORING/MONITORING AGENCY NAME(S) AND ADDRESS(ES) Air Force Research Laboratory Sensors Directorate Wright-Patterson Air Force Base, OH 45433-7320 Air Force Materiel Command United States Air Force			Defense Advanced Research Projects Agency DARPA/MTO 675 North Randolph Street Arlington, VA 22203		10. SPONSORING/MONITORING AGENCY ACRONYM(S) AFRL/RYDR	
					11. SPONSORING/MONITORING AGENCY REPORT NUMBER(S) AFRL-RY-WP-TR-2017-0164	
12. DISTRIBUTION/AVAILABILITY STATEMENT Approved for public release; distribution is unlimited.						
13. SUPPLEMENTARY NOTES This report is the result of contracted fundamental research deemed exempt from public affairs security and policy review in accordance with SAF/AQR memorandum dated 10 Dec 08 and AFRL/CA policy clarification memorandum dated 16 Jan 09. This material is based on research sponsored by Air Force Research laboratory (AFRL) and the Defense Advanced Research Agency (DARPA) under agreement number FA8650-16-1-7641. The U.S. Government is authorized to reproduce and distribute reprints for Governmental purposes notwithstanding any copyright notation herein. The views and conclusions contained herein are those of the authors and should not be interpreted as necessarily representing the official policies of endorsements, either expressed or implied, of Air Force Research Laboratory (AFRL) and the Defense Advanced Research Agency (DARPA) or the U.S. Government. Report contains color.						
14. ABSTRACT The objective of this program was to develop magneto-optical (MO) materials to enable nonreciprocal optical devices for the emerging standardized photonic integrated circuit (PIC) fabrication processes that include a range of optical and radio frequency (RF) photonic devices such as low-loss interconnect waveguides, power splitters, filters, as well as active amplifiers, lasers, optical modulators and photodetectors. Designs were made for resonator and Mach-Zehnder interferometer (MZI) isolator devices based on optical modeling, for both transverse-electric (TE) and transverse-magnetic (TM) polarization.						
15. SUBJECT TERMS magneto-optical devices, photonic integrated circuits, optical isolators, optical circulators						
16. SECURITY CLASSIFICATION OF:		17. LIMITATION OF ABSTRACT: SAR		18. NUMBER OF PAGES 15	19a. NAME OF RESPONSIBLE PERSON (Monitor) Dale Stevens	
a. REPORT Unclassified	b. ABSTRACT Unclassified	c. THIS PAGE Unclassified	19b. TELEPHONE NUMBER (Include Area Code) N/A			

Table of Contents

Section	Page
List of Figures	ii
1. Summary of Key Project Results.....	1
2. Research Description.....	2
3. Magneto-Optical Materials Development	3
4. Isolator Design.....	6
5. Waveguide Fabrication.....	7
6. Device Characterization	8
List of Abbreviations, Acronyms, and Symbols	10

List of Figures

Figure	Page
Figure 1: Single Crystal BiYIG/GGG	4
Figure 2: Polycrystalline Films on Si.....	5
Figure 3: Upper Panel: Top-view Optical Micrograph of the First Generation Fabricated Isolator Device and Lower Panel: Layout of MZI and Ring Resonator Waveguide Isolators, Edge- and Surface-Coupled Variants.....	6
Figure 4: Process Flow for SiNx-Waveguide Isolator Fabrication.....	7
Figure 5: (Left) Histogram showing Loaded Q-factor Distribution in Devices before and after Deposition of the BiYIG Layer near 1550 nm Wavelength (left) and TE Mode Resonant Peak Positions repeatedly Measured in Forward and Backward Directions (right)	8
Figure 6: TEM Image and (inset) Selected Area Electron Diffraction (SAED) Pattern of the Bi:YIG Film Deposited on Waveguide Sidewalls	9

1. Summary of Key Project Results

1. Growth process developed for bismuth garnet (BiYIG) on single crystal gallium gadolinium garnet ($\text{Gd}_3\text{Ga}_5\text{O}_{12}$ or GGG) and on silicon (Si) substrates. Films on Si were grown using a YIG seedlayer on top or underneath the BiYIG.
2. Optical, structural and composition characterization of BiYIG films showed that single crystal films behaved similarly to bulk in terms of magnetization and Faraday rotation (FR). Polycrystalline films on Si showed lower FR than expected which corresponded to lower Bi content than the target.
3. Designs were made for resonator and Mach-Zehnder interferometer (MZI) isolator devices based on optical modeling, for both transverse-electric (TE) and transverse-magnetic (TM) polarization.
4. Fabrication of resonator devices for TE isolation in Lincoln Laboratory (LL) Multi-Project Wafer (MPW) run.
5. Deposition of BiYIG/YIG and characterization of device performance were carried out. The insertion loss of order 7.5 dB is considerably improved over our prior devices (18.8 dB for 2011 publication and 13.5 dB in 2015) even though the devices were made by optical lithography with poorer dimensional control than electron-beam lithography patterned structures. Initial measurements of isolation ratio showed good performance but we found on repeated measurements that the nonreciprocal phase shift (NRPS) we had initially reported had actually originated in part from thermal drift during the measurement. Further testing showed a weak NRPS attributed to the short length of the window, the presence of a larger than expected gap between the magneto-optical material and the waveguide, and the low Bi content.
6. An additional wafer run is in progress to produce devices with larger windows and interferometer devices, and further work on stoichiometry control has enabled higher Bi content in the films. It is expected that these devices will give a measurable NRPS.

2. Research Description

The motivation for this work is two-fold: first of all, while most on-chip lasers emit in the TE polarization, our earlier isolator designs have exclusively operated with the TM polarization. In addition, our previously demonstrated isolator devices were fabricated using electron beam lithography patterning, which is not a scalable device manufacturing technique. The work was leveraged by support from LL through an Advanced Concepts Committee (ACC) 1 year seed project which ended on 12/31/2016. This enabled collaboration with LL in obtaining devices through a multi-project wafer run.

3. Magneto-Optical Materials Development

The magneto-optical (MO) oxide layer consists of $(\text{Bi}, \text{Y})_3\text{Fe}_5\text{O}_{12}$ or BiYIG, bismuth garnet. We selected this material because it has a better figure of merit than the CeYIG used in our prior work, especially at lower wavelengths (1310 nm vs. 1550 nm). We developed a top-down deposition process in which BiYIG/YIG stacks are grown on the Si waveguide with YIG on top. The stack is annealed at 800°C/5 min to crystallize both layers, with the YIG templating the BiYIG leading to garnet phases rather than other oxides, and the BiYIG is directly on the Si waveguide. Initial attempts led to a film with Bi oxide phases, because the Bi was in excess and could not escape during the anneal as occurs in Si/YIG/BiYIG stacks. Hence the composition was adjusted to include slightly more Fe which yielded films with only garnet peaks.

We developed conditions for growth of Bi-substituted iron garnet (BiYIG) on GGG garnet and Si substrates by combinatorial pulsed laser deposition.

For **single crystal films on GGG** (Figure 1) the conditions for growth that produced films with the best saturation magnetization (M_s) and surface topography were found to be at higher temperatures of 520-560°C and at oxygen pressures of 10 to 20 mTorr. Structural characterization revealed the growth of epitaxial BiYIG film on GGG without any secondary phases. This result was further confirmed by compositional analysis that showed the ratio of Bi+Y/Fe, as expected, was approximately 0.6 (in the range 0.62-0.65) suggesting no formation of secondary ferrous phases. The FR was 1.5 °/µm which is comparable to other work considering the Bi content. The saturation field for out of plane hysteresis or Faraday loops is ~2 kOe which is close to that expected just from shape anisotropy, i.e. magnetocrystalline or magnetoelastic contributions to anisotropy are probably small.

For **polycrystalline films on Si** (Figure 2) top-down crystallization of BiYIG using a YIG seed layer on topographical substrates was carried out to promote the crystallization of BiYIG on photonic substrates. A bilayer was grown (YIG/BiYIG/substrate) at 650°C then annealed at 800°C. With the top seed layer, Bi escape during annealing was suppressed and the composition had to be adjusted (less Fe was added) to avoid secondary phases. X-ray diffraction (XRD) showed crystallization to the garnet structure and the saturation magnetization was consistent with the film thickness and the bulk magnetization of YIG and BiYIG (which are similar). However, films on Si had much weaker FR than expected. During this work, the pulsed-laser deposition (PLD) system was reconfigured leading to a higher intensity of light incident on the target and higher growth rates, which led to a change in composition of most materials deposited by PLD. Compositional analysis showed that more recent BiYIG films contained less Bi than before, and this may account for the lower FR. The target, which contained $\text{Bi}:\text{Y}:\text{Fe} = 0.8:2.2:5$, yielded films of 0.5:2.5:3.8, or 0.5:1.9:4.2 when additional Fe oxide was codeposited. (In the latter case, $\text{Bi}+\text{Y}/\text{Fe} = 0.57$ which matches the stoichiometric ratio of $3/5 = 0.6$.)

The results of growth experiments indicate that films grow with garnet crystal structure on GGG, even if the Bi+Y/Fe stoichiometry is not exactly correct. However, growth on Si is less forgiving, and making good quality garnet requires a closer control of stoichiometry. The Bi:Y ratio is controlled mainly by temperature, and the Bi+Y/Fe ratio is sensitive to laser power.

Sidewall growth. The TE mode device design in the LL MPW run requires the MO material to

be grown on the sidewall of the waveguide (see Figure 2). An angled deposition process was developed to obtain reasonable growth rates on the sidewall.

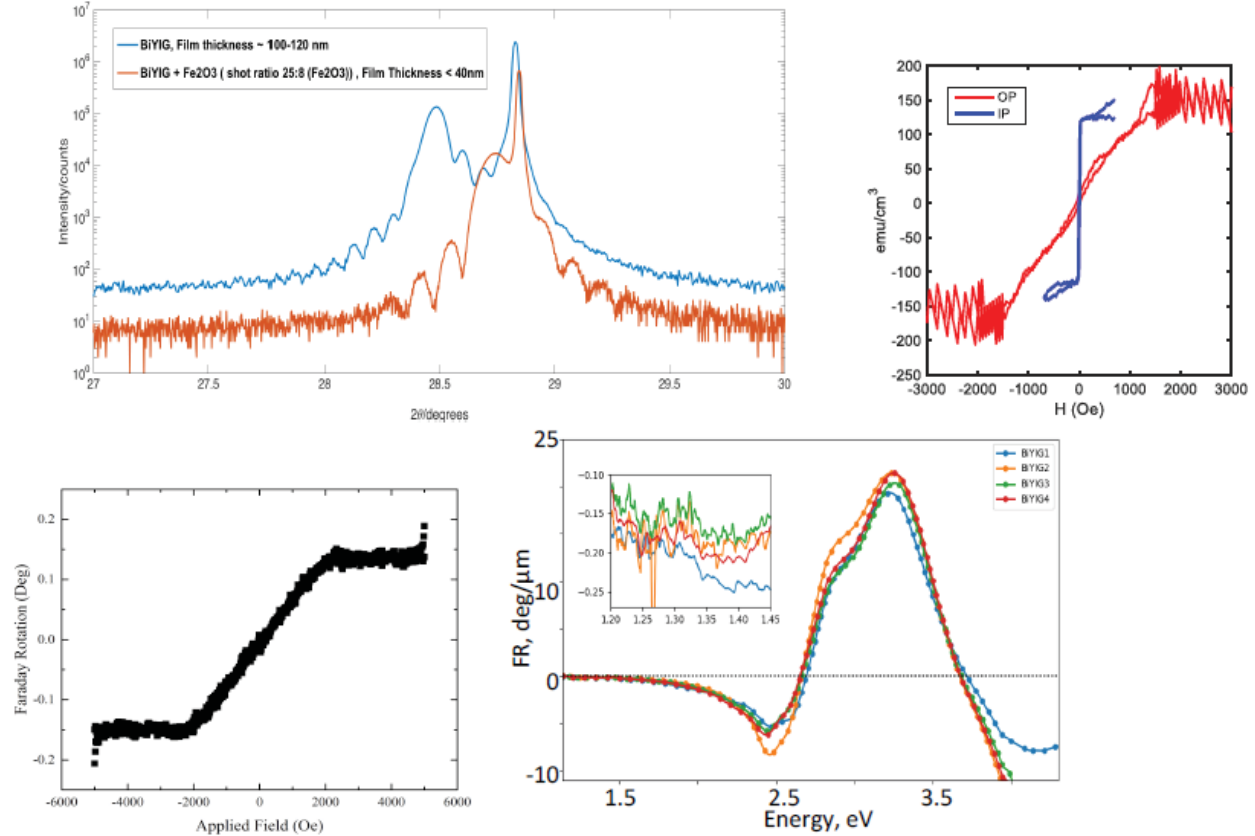
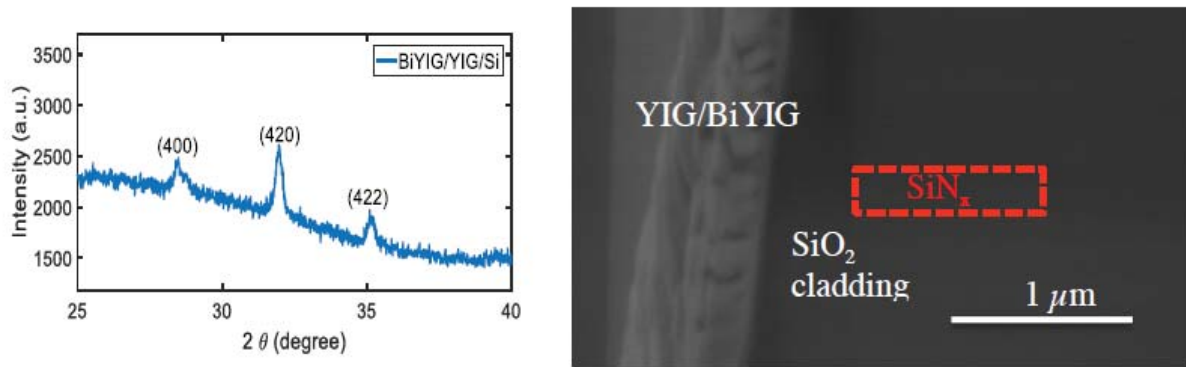


Figure 1: Single Crystal BiYIG/GGG

Top left: XRD of two recent films on (111) GGG showing the effect of adding Fe. Right: Magnetometry data showing in plane (IP) and out of plane (OP) hysteresis loops for 100 nm thick Bi_{0.97}Y_{2.47}Fe₅O₁₂ grown at 560°C, 20mTorr, 400mJ, on GGG (111). Lower left: OP Faraday loop of same film. Right: FR vs wavelength, in agreement with measurements on bulk BiYIG.



LL MPW fabrication process

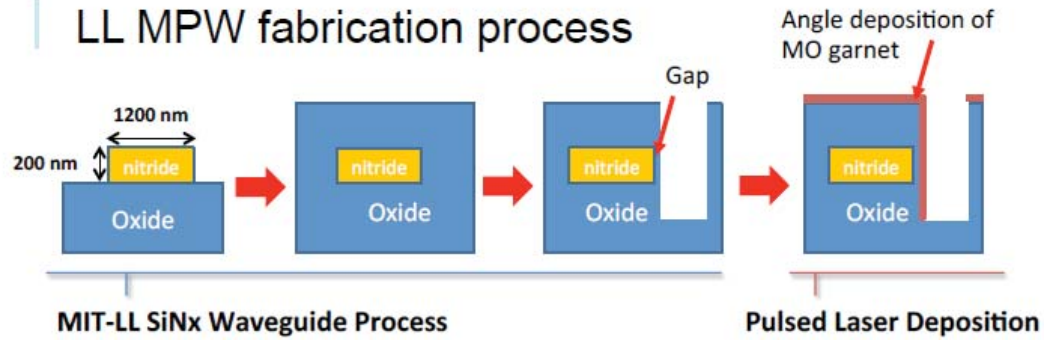


Figure 2: Polycrystalline Films on Si

Left: XRD of polycrystalline BiYIG film on Si grown with YIG bottom seed layer, showing the characteristic garnet peaks. Right: Scanning electron microscopy (SEM) of BiYIG grown on the sidewall of a SiN waveguide in a TE-mode isolator. The fabrication of the TE mode isolator is shown in the schematic.

4. Isolator Design

An example of a first generation isolator, made at LL, is shown in Figure 3 upper panel. Device performance will be described below. Devices were designed for an optical wavelength of $1.3\mu\text{m}$. There are designs for both TE and TM polarizations for ring resonators and Mach Zehnder designs (lower panel). Due to space constraints on the multi-project wafer, designs for only one wavelength were produced.

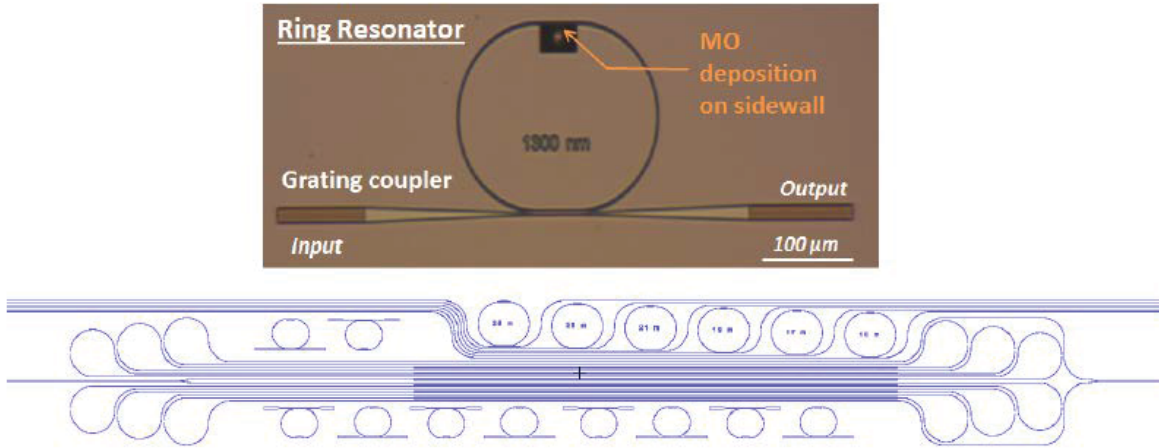


Figure 3: Upper Panel: Top-view Optical Micrograph of the First Generation Fabricated Isolator Device and Lower Panel: Layout of MZI and Ring Resonator Waveguide Isolators, Edge- and Surface-Coupled Variants

5. Waveguide Fabrication

The multi-project wafer fabrication process flow was designed. The fabrication requires only one etch step unique to the isolator structure. (Fabrication sequences were also adapted for processing devices made using electron beam lithography.)

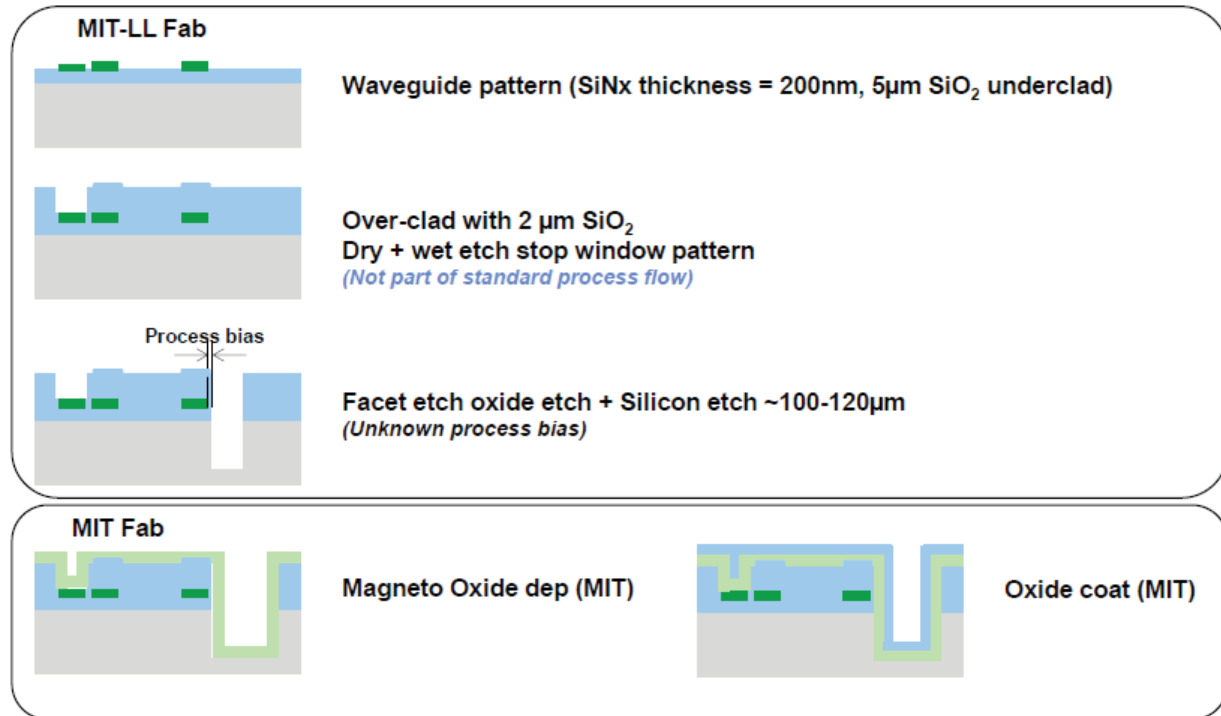


Figure 4: Process Flow for SiNx-Waveguide Isolator Fabrication

6. Device Characterization

Figure 5 shows a top view optical micrograph of the fabricated device. As can be seen from the figure, an oxide window is etched into the oxide cladding next to the ring resonator waveguide. Figure 5 (left) is a histogram showing the distribution of loaded Q-factors measured in devices before and after deposition of the BiYIG layer near 1550 nm wavelength. The devices exhibit loaded Q-factors of about 30,000 prior to BiYIG deposition, which corresponds to an equivalent propagation loss of ~ 5 dB/cm. This number is much higher than the baseline SiN_x waveguide loss of 0.2-0.3 dB/cm, and we attribute the excess loss to: 1) optical scattering occurring at the abrupt junction between the oxide window and the other parts of the resonator, which accounts for 4.6 dB/cm equivalent linear loss (0.17 dB per junction); and 2) radiative loss from a straight to a bent waveguide segment, which results in 1.1 dB/cm equivalent linear loss (0.02 dB per junction).

Performance of the isolator devices were quantified by comparing the forward and backward transmission spectra. Figure 5 (right) shows the measured resonant peak positions for the device (measurement repeated 6 times). No measurable nonreciprocal resonance shift was observed within the measurement error (~ 1 pm, limited by temperature fluctuations). [Note: preliminary measurements on several devices had shown a NRPS, but this was attributed later to thermal effects when measurements were repeated.]

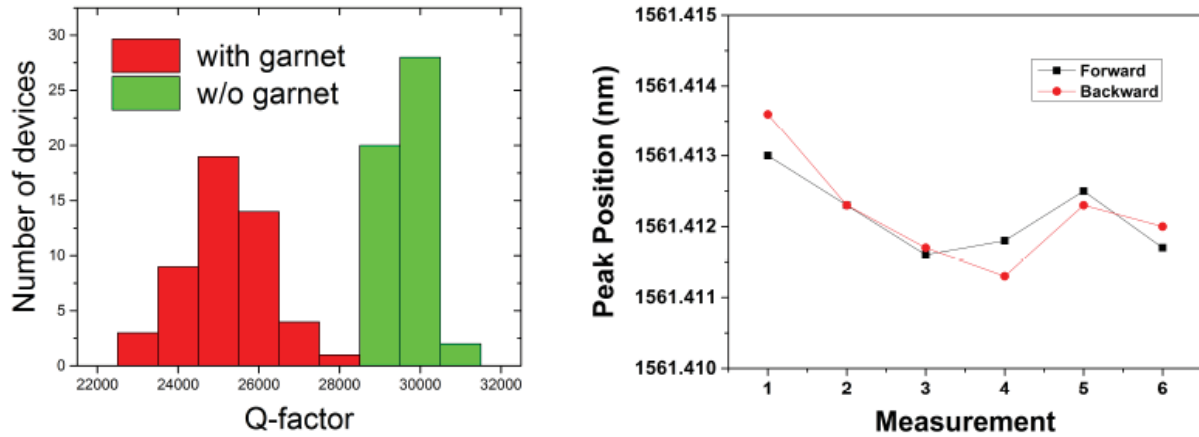


Figure 5: (Left) Histogram showing Loaded Q-factor Distribution in Devices before and after Deposition of the BiYIG Layer near 1550 nm Wavelength (left) and TE Mode Resonant Peak Positions repeatedly Measured in Forward and Backward Directions (right)

To diagnose the possible causes for the absence of NRPS, we performed optical simulations on the device structure. We found that for an assumed FR value of 1,000 dB/cm, the device design should yield a nonreciprocal resonance shift of 2.1 pm. We therefore estimate that the FR value in the BiYIG films on the sidewall is likely much less than the estimated 1,000 dB/cm value. We performed transmission electron microscopy (TEM) analysis on the BiYIG films (Figure 6) and found that they are fully crystallized. Therefore, it is possible that Bi was not fully incorporated into the sidewall layers as we had expected or that the Bi content is lower than films grown previously. Compositional analysis in films on flat substrates indicated a Bi content lower than expected. We revised our device design to 1) incorporate a longer window section; 2) include a

Bezier curve between the bent waveguides and the straight sections to reduce radiative loss; and 3) add a taper region to minimize the scattering loss between waveguide segments with and without the magnetic oxide sidewall coverage. The new devices are currently being processed through LL's MPW run and will be coated with BiYIG and characterized in the next months.

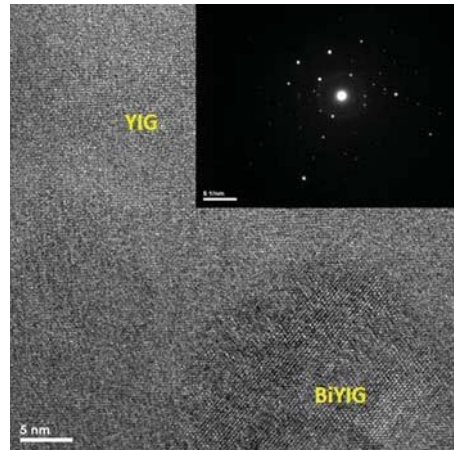


Figure 6: TEM Image and (inset) Selected Area Electron Diffraction (SAED) Pattern of the Bi:YIG Film Deposited on Waveguide Sidewalls
Both TEM observation and SAED pattern suggest full crystallization.

List of Abbreviations, Acronyms, and Symbols

ACRONYM	DESCRIPTION
ACC	Advanced Concepts Committee
BiYIG	bismuth garnet
FR	Faraday rotation
Gd ₃ Ga ₅ O ₁₂ or GGG	gallium gadolinium garnet
IP	in plane
LL	Lincoln Laboratory
MO	magneto-optical
MPW	Multi-Project Wafer
Ms	saturation magnetization
MZI	Mach-Zehnder interferometer
NRPS	nonreciprocal phase shift
OP	out of plane
PLD	pulsed-laser deposition
SAED	selected area electron diffraction
SEM	scanning electron microscopy
Si	silicon
TE	transverse-electric
TEM	transmission electron microscopy
TM	transverse-magnetic
XRD	X-ray diffraction